AIP | Applied Physics Letters

Application of proton boron fusion reaction to radiation therapy: A Monte Carlo simulation study

Do-Kun Yoon, Joo-Young Jung, and Tae Suk Suh

Citation: Applied Physics Letters **105**, 223507 (2014); doi: 10.1063/1.4903345
View online: http://dx.doi.org/10.1063/1.4903345
View Table of Contents: http://scitation.aip.org/content/aip/journal/apl/105/22?ver=pdfcov
Published by the AIP Publishing

APPLIED PHYSICS LETTERS **105**, 223507 (2014)

Application of proton boron fusion reaction to radiation therapy: A Monte Carlo simulation study

Do-Kun Yoon, Joo-Young Jung, and Tae Suk Suh[a)]
Department of Biomedical Engineering and Research Institute of Biomedical Engineering, College of Medicine, Catholic University of Korea, Seoul 505, South Korea

(Received 30 July 2014; accepted 20 November 2014; published online 2 December 2014)

Three alpha particles are emitted from the point of reaction between a proton and boron. The alpha particles are effective in inducing the death of a tumor cell. After boron is accumulated in the tumor region, the emitted from outside the body proton can react with the boron in the tumor region. An increase of the proton's maximum dose level is caused by the boron and only the tumor cell is damaged more critically. In addition, a prompt gamma ray is emitted from the proton boron reaction point. Here, we show that the effectiveness of the proton boron fusion therapy was verified using Monte Carlo simulations. We found that a dramatic increase by more than half of the proton's maximum dose level was induced by the boron in the tumor region. This increase occurred only when the proton's maximum dose point was located within the boron uptake region. In addition, the 719 keV prompt gamma ray peak produced by the proton boron fusion reaction was positively detected. This therapy method features the advantages such as the application of Bragg-peak to the therapy, the accurate targeting of tumor, improved therapy effects, and the monitoring of the therapy region during treatment. © *2014 AIP Publishing LLC*.
[http://dx.doi.org/10.1063/1.4903345]

Proton boron fusion reaction has been investigated through the nuclear physics research since 1960. After the proton reacts with the boron (^{11}B), the boron changes to carbon (^{12}C) in an excited state. The excited carbon nucleus is split into alpha particle of 3.76 MeV and beryllium (^{8}Be). Subsequently, the beryllium is divided into the two alpha particles of 2.74 MeV each.[1–4] The principle of the proton boron fusion therapy (PBFT) is based on this reaction as the radiation therapy technique. In the case of boron neutron capture therapy (BNCT), after the thermal neutron was captured by the labeled boron in the tumor region, an alpha particle is emitted from the capture reaction point.[5] An alpha particle induces the death of the tumor cell by the one capture reaction.[6] However, three alpha particles are emitted from the point of the proton boron fusion reaction. If this reaction is applied to the radiation therapy, the therapy results could be more effective in inducing the death of tumor cells using a smaller flux. In addition, the proton's energy loss during its propagation through matter is described by the Bragg-peak.[7–10] After the boron-labeled compound is accumulated in the tumor region, if the portion of the proton's maximum dose (Bragg-peak) is included at the tumor region, which is the boron uptake region (BUR), a dramatic therapy effect with less damage to normal tissue can be expected. First, because three alpha particles can contribute to the death of the tumor cell by the use of one proton, high therapy efficiency can be achieved by using smaller flux than conventional proton therapy or the BNCT. Naturally, the proton's maximum dose level point should be included in the BUR.[11] Second, the proton boron fusion reaction induces a prompt gamma ray from the reaction point. When this single prompt photon is detected using a gamma camera or a single photon emission computed tomography (SPECT), the therapy region can be monitored during PBFT.[12,13] In this study, we present the introduction of a therapy method using the proton boron fusion reaction. The purpose of this study is to verify the theoretical validity of PBFT using Monte Carlo simulations. Figure 1 is a

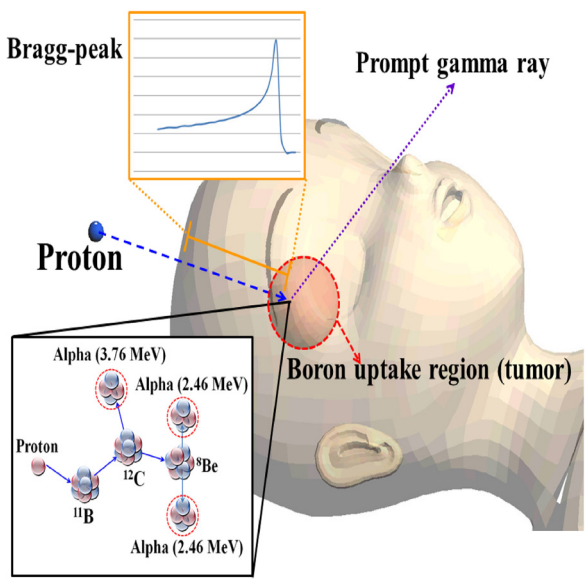

FIG. 1. Conceptual diagram of PBFT. The proton reacts with the boron in the tumor region. After the reaction, three alpha particles kill the tumor cell, and the maximum point of the Bragg-peak is increased by the boron at the BUR. In addition, the prompt gamma ray emitted by the reaction can provide information about the therapy region.

[a)]Author to whom correspondence should be addressed. Electronic mail: suhsanta@catholic.ac.kr. Tel.: +82-2-2258-7232. Fax: +82-2-2258-7506. Present address: Department of Biomedical Engineering, College of Medicine, The Catholic University of Korea, 222 Banpo-daero, Seocho-gu, Seoul 137-701, South Korea.

schematic diagram of the PBFT principle, which was described at previous part.

To verify the theoretical validity of PBFT, the Monte Carlo n-particle extended (MCNPX, Ver.2.6.0, LANL, New Mexico, USA) simulation code was used. In this study, there are three parts of the simulation to confirm the validity of PBFT. First, the variation of the Bragg-peak of the proton depending on the location of the BUR was examined. Second, when the proton's maximum dose level point is involved at the BUR, the variation of the maximum dose level according to the proton energy was evaluated. The last simulation was performed to confirm the existence of the prompt gamma ray peak of 719 keV from energy spectrum simulation.

For the first simulation study, a water phantom with cylindrical geometry (density: 1 g/cm^3, diameter: 16 cm, and height: 6 cm) was used and an 80 MeV proton beam (flux: 40 000 000 particles/cm^2·s) was emitted at 50 cm distance from water surface.[14] In order to induce the reaction effectively, we used a default dataset of reaction cross section in the MCNPX simulation without any changing of reaction cross section. After the acquisition of the percentage depth dose (PDD) of the proton in the water phantom without the BUR using the F6 tally (absorbed dose tally), the BUR (purity of Boron (^{11}B): 100%, density: 2.08 g/cm^3) was inserted in the water phantom. The geometry of the BUR was cylindrical with a 6 cm diameter and 0.8 cm height.[15] The boron concentration can be estimated by the density and size of the BUR. The concentration of the boron can influence to the reaction rate significantly. Two BURs were used, with centers located at 0.8 cm and 5.2 cm below the water surface. Because the Bragg-peak of the 80 MeV proton beam was located between 4.8 cm and 5.4 cm below the water surface, the BUR agreed with that range.[8,13] The two corresponding PDDs were compared with the general proton's PDD from the water phantom without the BUR. When the location of the BUR was fixed, the PDDs of the 80 MeV and 90 MeV proton beam were acquired to set as the testing group. For the dose calculation at each depth, the water phantom was divided into 30 segments of 0.2 cm thickness. Basically, all results of PDD were acquired using the F6 tally (absorbed dose tally, unit: MeV/g). However, the counting of additional proton by the alpha particle is based on the results by using F4 tally (flux tally, unit: particles/cm^2). The variation amount of area under fluence graph was considered to the proton's PDD by the conversion of percentage.[7] Also, in order to observe the amplification of the proton's maximum dose level at the axial view, dose profiles from the water and BUR were acquired. The proton dose was measured at a perpendicular line to the proton's maximum dose level point in the PDD. Basically, the dose profile of the proton with the natural conditions was normalized using same method which is used for a conventional proton therapy. The amplification degree of the proton's maximum dose level at the BUR was demonstrated with the normalization based on the proton dose in the water without the BUR.

In the second simulation, in order to confirm the increase of the maximum point of the Bragg-peak depending on the energy, proton sources of three different energies (80 MeV, 90 MeV, and 100 MeV) were used.[10] Because the increase of the proton energy causes the increase of the Bragg-peak range, water phantom greater heights were required to deduce the PDD without the cut-off. The height of the water phantom was extended up to 10 cm with the same diameter, and each location of the BUR was adjusted to include the proton's maximum dose level point according to the three different energies. The centers of the three different BURs were located at 5.2 cm, 6.4 cm, and 7.8 cm, respectively, below the water surface.

When PBFT is applied to the clinical case, the monitoring of the treated region adds to the effectiveness of the therapy. In order to find the effective prompt gamma ray peak for the imaging, the energy spectra were acquired using the F8 tally (energy deposition tally) in MCNPX.[12,16–19] When the proton beam passed through the water phantom, with and without the BUR, the induced prompt gamma rays were counted by the external high purity germanium detector (HPGe, density: 5.32 g/cm^3) according to their energy.[20] This semiconductor material was the cylindrical-shell type with a 150 cm inner diameter and a 10 cm thickness.[21]

The simulation results show the basic application feasibility of PBFT. Figure 2(a) shows the variation of PDD depending on the location of the BUR. The black line is the PDD of the 80 MeV proton beam in the water phantom without the BUR. The maximum dose level point appeared at approximately 5.2 cm, and this dose level was assigned as 100% value for the calibration of the other simulation results.[7] The blue line denotes the PDD of the proton in the water phantom including the BUR, which was displaced from the proton's maximum dose level point. Although the BUR was included in the water, the maximum dose level of the proton did not exceed 100%. In addition, the dose level of the proton was increased by the reaction with the boron at the BUR, and the increased range is similar to the range of the BUR. The red line shows the proton's PDD when the proton's maximum dose level point is located within the BUR. Basically, the proton's maximum dose level point is not increased under any circumstance.[14] However, the result definitely shows the increase of the maximum dose level. This indicates the possibility of more effective delivery of the critical dose to the tumor, as well as a dramatic reduction of the proton flux used for therapy by the boron. This impact is based on the reaction cross section between the proton and boron. Naturally, when the boron concentration is below the particular value (same size with below 1 g/cm^3 density), although the proton boron fusion reaction occurred, the proton's maximum dose level could be below natural maximum level (relative dose: 100%). There is one more outcome regarding the effectiveness of the method, the agreement between the BUR and proton's maximum dose level point (Figure 2(b)). When the center of the location of the BUR was fixed at 5.2 cm below the water surface, the PDDs of the proton (80 MeV and 90 MeV) were acquired. Because the location of the BUR was adjusted to the maximum dose level point of the 80 MeV proton beam, an increase of the maximum dose level of the 80 MeV proton beam was observed. However, the maximum dose level of the 90 MeV proton beam exceeded the BUR by 0.8 cm. In the case of the PDD of the 90 MeV proton beam, although the BUR was located at the nearby maximum dose level point, no increase of the

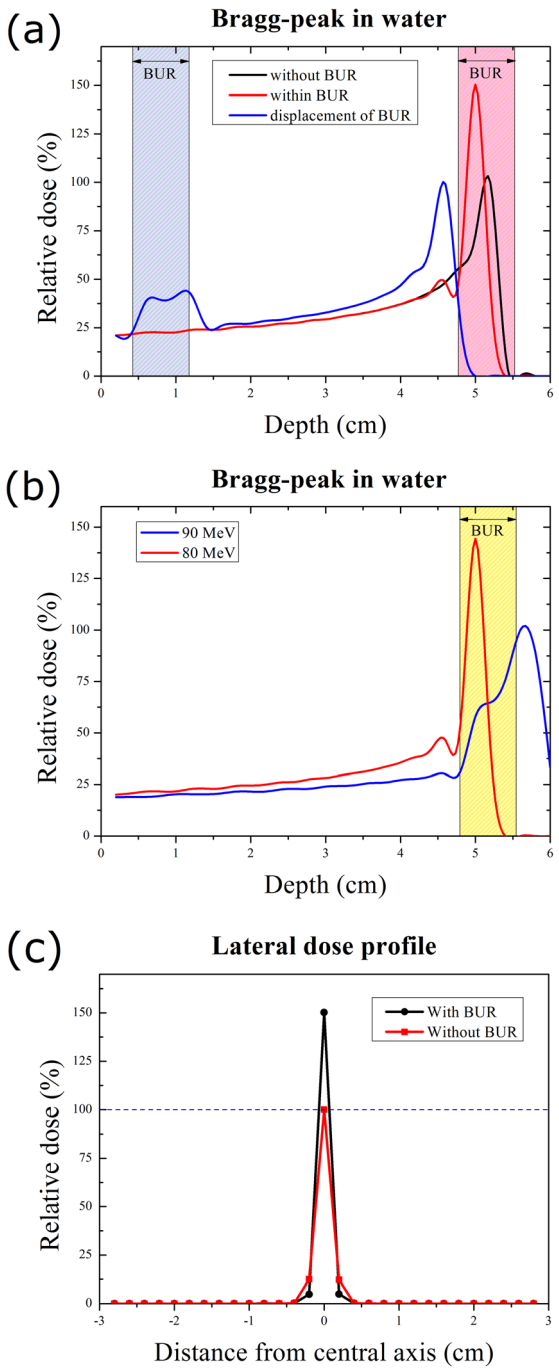

FIG. 2. PDD of the proton from the water phantom with variable conditions. (a) PDD for the three examined cases of the 80 MeV proton; the black line is the normalized PDD from the water phantom without the BUR, the blue line shows the PDD from the water phantom when the BUR is displaced from the proton's maximum dose level point, and the red line is the PDD from the water phantom when the proton's maximum dose level point is located within the BUR. (b) PDD of the proton according to the energy, using the water phantom including the fixed BUR (red line: 80 MeV proton, blue line: 90 MeV proton). (c) Dose profiles of the proton; the red line is a proton dose profile in the water without the BUR, the black line shows the amplified proton dose profile in the BUR.

maximum dose level appeared in the Bragg-peak curve. From these results, when the treatment planning is performed for the PBFT, the physicist should consider the impact of proton range degradation from 0.1 cm to 0.3 cm. There are two characteristic in the dose profile of the proton (Figure 2(c)). The red line is the normalized dose profile of the proton in the water without the BUR, and the black line shows the amplified relative dose profile of the proton at the BUR. First, there is an increase of the proton dose as we had anticipated clearly. Another characteristic is the variation of the dose at the area of penumbra. The impact by the penumbra was decreased by using PBFT method. These two characteristics can be helpful to the therapy effect certainly.

Figure 3 shows the PDDs of the three energies ((a): 80 MeV, (b): 90 MeV, and (c): 100 MeV). The PDD in the water without the BUR was used as the reference. The increments of the maximum dose level were 50.5%, 50.9%, and 79.5%, respectively. An increase by more than a half was reported for all three cases. Moreover, the resulting

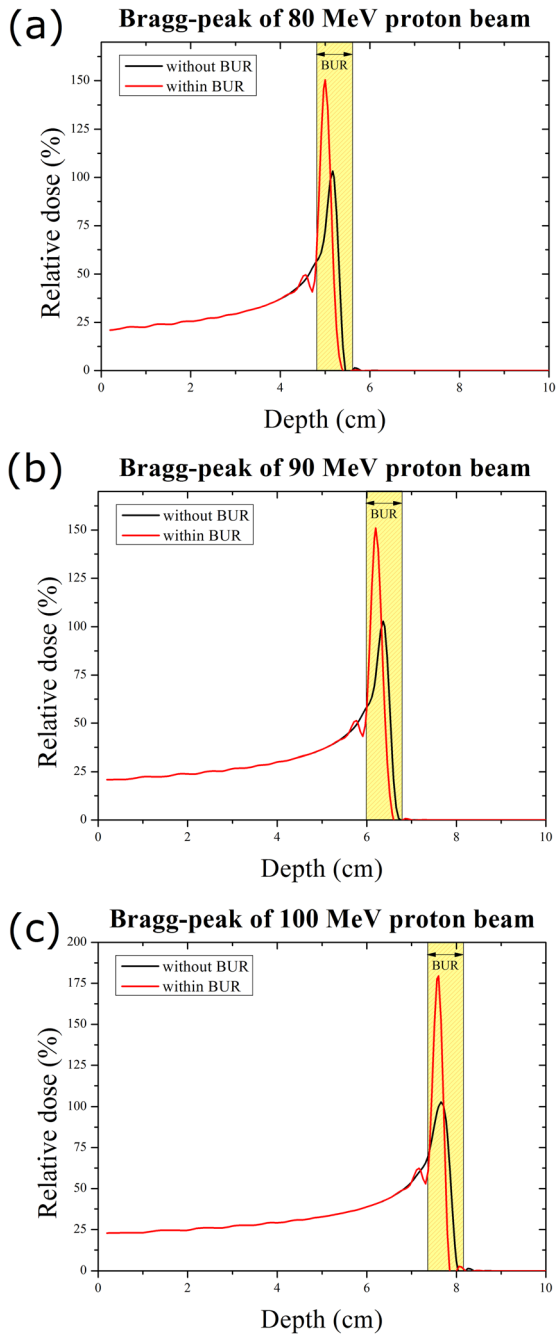

FIG. 3. PDDs with relation to the energy deposited in the water phantom. The center of the BUR was adapted to each proton's maximum dose level point. The PDD which shows increased dose level in the BUR (red line) was superposed on the normalized PDD (black line). The proton energies were 80 (a), 90 (b), and 100 MeV (c).

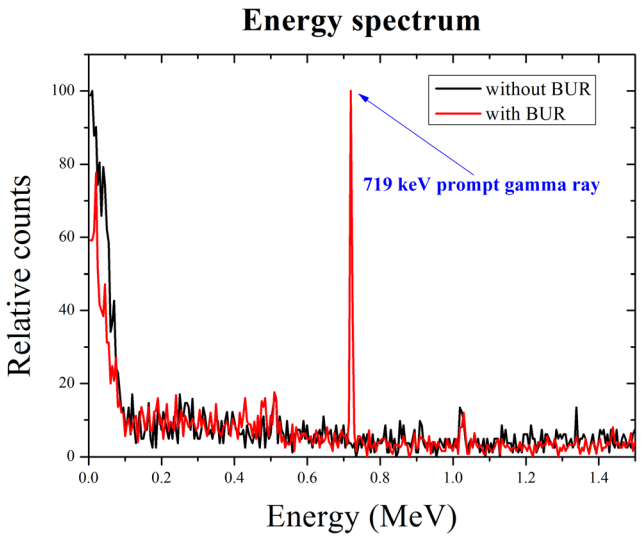

FIG. 4. Energy spectrum of the prompt gamma ray by the proton boron fusion reaction. The black line denotes the spectrum when the BUR was excluded from the water phantom. The red line shows the spectrum when the water phantom includes the BUR. The prompt gamma ray peak of 719 keV undeniably appears in the spectrum.

maximum dose level points were almost the same as the original points. This dramatic increase of the maximum dose level can induce more effective damage to the tumor cell. In addition, although the location of the BUR was changed, the increased maximum dose level could be maintained during a change of the proton energy. However, because the effectiveness of this method ultimately depends on the reaction cross section, in order to apply to the clinical effectiveness, the increase of the reaction cross section is critical. From all results, the falling off of dose at the boundary between the BUR and water was shown. It means that when the incident proton is captured at the ^{11}B, the number of counted proton at each slab (geometry in simulation) is relatively small at the boundary because of the fusion reaction. Also, there is no additional proton by the generation of the alpha particle from the water portion. In this simulation study, because the code setting includes the proton source with the proton tally, this setting makes it difficult to distinguish the reason of an increase of the proton dose by the generation of the alpha particle. If the boron neutron capture reaction is simulated with the neutron source and the proton tally, the variation of the proton dose by the alpha particle can be observed clearly. Also, actually the MCNPX code can simulate the proton boron fusion reaction with the basic reaction cross section data. The reason of the increase in the peak-to-plateau is not just a result of an increase in density.

In order to confirm the existence of the prompt gamma ray induced by the proton boron reaction, the simulations of two cases were performed. Figure 4 shows the energy spectrum of the prompt gamma ray obtained by the simulations. The black line is the spectrum of the prompt gamma ray from the water phantom without the BUR, which contains no characteristic peak. However, when the BUR was included in the water phantom, a distinct prompt gamma ray peak appears in the spectrum by the simulation using identical conditions as in the previous simulation. The number of counts in the 719 keV prompt gamma ray peak was sufficiently high for identification. If an event from the prompt gamma ray is detected during the irradiation of the proton beam, the therapy site can be observed during PBFT.

Because the PBFT method is still at the conceptual stage, the verification of its effectiveness is required for the use of a physical approach. Naturally, although further verification must be obtained for the clinical application of the method, its fundamental effectiveness and advantages have been verified by our results. In the future study, an experiment based on the current phantom study will be conducted as the next step toward the application of PBFT in the clinical field.

This research was supported by Leading Foreign Research Institute Recruitment Program through the National Research Foundation of Korea (NRF) funded by the Ministry of Science, Information and Communication Technologies (ICT) and Future Planning (MSIP) (Grant No. 2009−00420) and the Radiation Technology Research and Development program (Grant No. 2013043498), Republic of Korea.

[1]C. Labaune, C. Baccou, S. Depierreux, C. Goyon, G. Loisel, V. Yahia, and J. Rafelski, Nat. Commun. **4**, 2506 (2013).
[2]J. M. Martinez-Val, S. Eliezer, M. Piera, and G. Velarde, Phys. Lett. A **216**(1), 142 (1996).
[3]D. C. Moreau, Nucl. Fusion **17**(1), 13 (1977).
[4]B. Levush and S. Cuperman, Nucl. Fusion **22**(11), 1519 (1982).
[5]T. Kobayashi, Y. Sakurai, and M. Ishikawa, Med. Phys. **27**(9), 2124 (2000).
[6]V. A. Nievaart, D. Légrà dy, R. L. Moss, J. L. Kloosterman, T. H. J. J. van der Hagen, and H. van Dam, Med. Phys. **34**(4), 1321 (2007).
[7]M. R. Akbari, H. Yousefnia, and E. Mirrezaei, Appl. Radiat. Isot. **90**, 89 (2014).
[8]E. Testa, M. Bajard, M. Chevallier, D. Dauvergne, F. Le Foulher, N. Freud, J. M. Létang, J. C. Poizat, C. Ray, and M. Testa, Appl. Phys. Lett. **93**(9), 093506 (2008).
[9]C. H. Min, C. H. Kim, M. Y. Youn, and J. W. Kim, Appl. Phys. Lett. **89**(18), 183517 (2006).
[10]S. Shimizu, T. Matsuura, M. Umezawa, K. Hiramoto, N. Miyamoto, K. Umegaki, and H. Shirato, Phys. Med. **30**(5), 555 (2014).
[11]S. J. Frank, J. D. Cox, M. Gillin, R. Mohan, A. S. Garden, D. I. Rosenthal, G. B. Gunn, R. S. Weber, M. S. Kies, J. S. Lewin, M. F. Munsell, M. B. Palmer, N. Sahoo, X. Zhang, W. Liu, and X. R. Zhu, Int. J. Radiat. Oncol. Biol. Phys. **89**(4), 846 (2014).
[12]D. Yoon, J. Jung, K. J. Hong, and T. S. Suh, Appl. Phys. Lett. **104**(8), 083521 (2014).
[13]M. S. Park, W. Lee, and J. M. Kim, Appl. Phys. Lett. **97**(15), 153705 (2010).
[14]H. Noshad and N. Givechi, Radiat. Meas. **39**(5), 521 (2005).
[15]F. Rahmani and M. Shahriari, Ann. Nucl. Energy **38**(2–3), 404 (2011).
[16]B. J. Min, Y. Choi, N. Y. Lee, J. H. Jung, K. J. Hong, J. Kang, W. Hu, and Y. B. Ahn, Nucl. Instrum. Methods Phys. Res., Sect. A **633**(1), 61 (2011).
[17]R. Khelifi, V. A. Nievaart, P. Bode, R. L. Moss, and G. C. Krijger, Appl. Radiat. Isot. **67**(7–8), S359 (2009).
[18]D. M. Minsky, A. A. Valda, A. J. Kreiner, S. Green, C. Wojnecki, and Z. Ghani, Appl. Radiat. Isot. **69**(12), 1858 (2011).
[19]I. Jun, W. Kim, M. Smith, I. Mitrofanov, and M. Litvak, Nucl. Instrum. Methods Phys. Res., Sect. A **629**(1), 140 (2011).
[20]P. A. Söderström, F. Recchia, J. Nyberg, A. Al-Adili, A. Ataç, S. Aydin, D. Bazzacco, P. Bednarczyk, B. Birkenbach, D. Bortolato, A. J. Boston, H. C. Boston, B. Bruyneel, D. Bucurescu, E. Calore, S. Colosimo, F. C. L. Crespi, N. Dosme, J. Eberth, E. Farnea, F. Filmer, A. Gadea, A. Gottardo, X. Grave, J. Grebosz, R. Griffiths, M. Gulmini, T. Habermann, H. Hess, G. Jaworski, P. Jones, P. Joshi, D. S. Judson, R. Kempley, A. Khaplanov, E. Legay, D. Lersch, J. Ljungvall, A. Lopez-Martens, W. Meczynski, D. Mengoni, C. Michelagnoli, P. Molini, D. R. Napoli, R. Orlandi, G. Pascovici, A. Pullia, P. Reiter, E. Sahin, J. F. Smith, J. Strachan, D. Tonev, C. Unsworth, C. A. Ur, J. J. Valiente-Dobón, C. Veyssiere, and A. Wiens, Nucl. Instrum. Methods Phys. Res., Sect. A **638**(1), 96 (2011).
[21]K. J. Hong, Y. Choi, J. H. Jung, J. Kang, W. Hu, H. K. Lim, Y. Huh, S. Kim, J. W. Jung, K. B. Kim, M. S. Song, and H. W. Park, Med. Phys. **40**(4), 042503 (2013).